

Direct Wiring of Liquid Metal on an Ultrasoft Substrate Using a Polyvinyl Alcohol Lift-off Method

Koki Murakami, Ryota Tochinai, Daiki Tachibana, Yuji Isano, Ryosuke Matsuda, Fumika Nakamura, Yuta Kurotaki, Yutaka Isoda, Monami Yamane, Yuya Sugita, Junji Fukuda, Kazuhide Ueno, Norihisa Miki, Ohmi Fuchiwaki,* and Hiroki Ota*



Cite This: <https://doi.org/10.1021/acsami.1c20628>



Read Online

ACCESS |



Metrics & More



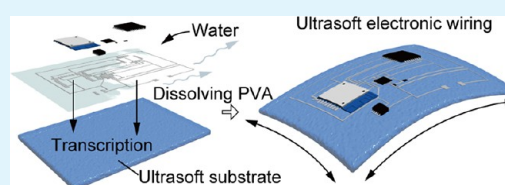
Article Recommendations



Supporting Information

ABSTRACT: In recent years, wiring and system construction on ultrasoft materials such as biological tissues and hydrogels have been proposed for advanced wearable devices, implantable devices, and soft robotics. Among the soft conductive materials, Ga-based liquid metals (LMs) are both biocompatible and ultrasoft, making them a good match for electrodes on the ultrasoft substrates. However, gels and tissues are softer and less wettable to the LMs than conventional soft substrates such as Ecoflex and polydimethylsiloxane. In this study, we demonstrated the transfer of LM paste composed of Ga-based LM and Ni nanoparticles onto ultrasoft substrates such as biological tissue and gels using sacrificial polyvinyl alcohol (PVA) films. The LM paste pattern fabricated on the PVA film adhered to the ultrasoft substrate along surface irregularities and was transferred without being destroyed by the PVA film before the PVA's dissolution in water. The minimum line width that could be wired was approximately 165 μm . Three-dimensional wiring, such as the helical structure on the gel fiber surface, is also possible. Application of this transfer method to tissues using LM paste wiring allowed the successful stimulation of the vagus nerve in rats. In addition, we succeeded in transferring a temperature measurement system fabricated on a PVA film onto the gel. The connection between the solid-state electrical element and the LM paste was stable and maintained the functionality of the temperature-sensing system. This fundamental study of wiring fabrication and system integration can contribute to the development of advanced electric devices based on ultrasoft substrates.

KEYWORDS: liquid metal, hydrogel, polyvinyl alcohol, transfer, soft electronics



1. INTRODUCTION

Smart and flexible devices have been produced based on thick films of silicone rubber, such as polydimethylsiloxane (PDMS) and Ecoflex, as flexible substrates.^{1–3} To improve flexibility, ultrathin films of polyurethane, PDMS, Parylen, and poly(styrene-butadiene-styrene) triblock copolymer (SBS) were used as substrates. Furthermore, in recent years, the implementation of devices on softer materials such as hydrogels and biological tissue has become essential for use in the next generation of smart devices.^{4,5} For example, direct wiring of biological tissues is applied in implants and in vivo electronic monitoring. In addition, wiring and system configurations with gels that are softer than biological tissues (Young's modulus of 10^3 to 10^6 Pa)⁶ have been proposed and are expected to be used in medical and biological applications.^{7,8} Hydrogel, a polymer material with a Young's modulus of 10^3 to 10^5 Pa and with properties intermediate to those of liquids and solids, is softer than silicone rubbers and can be used as an ultrasoft and ultra-adhesive substrate because it can easily fit and adhere to complex shapes.^{9,10}

Silver nanocomposites,¹¹ poly(3,4-ethylenedioxythiophene) poly(styrenesulfonate) (PEDOT:PSS),¹² and carbon nanotubes (CNTs)¹³ have been proposed as flexible wiring (conductive) materials on ultrasoft materials such as hydrogels.

In this study, we focused on Ga-based liquid metals (LMs) such as eutectic GaIn (EGaIn) and Galinstan as one of these conductive materials. In particular, Galinstan is a biocompatible material with a melting point of -19 °C, a viscosity of 2.4 mPa · s, and a specific gravity of 6.44 g/cm³.^{14,15} Ga-based LMs have been used for wiring parts,¹⁶ sensor reaction parts,¹⁷ and connections with different conductive materials¹⁸ of flexible and stretchable devices. Although Ga-based LMs have the drawback of being difficult to handle compared with conventional conductive materials, it has advantages in that its Young's modulus is lower than that of gels, and its stretchability is high, which does not prevent the deformation of the substrates. In addition, the resistance change due to the deformation is small. Therefore, Ga-based LMs are conductive materials that are highly compatible with ultrasoft materials such as biological tissues and hydrogels.

Received: October 26, 2021

Accepted: January 19, 2022

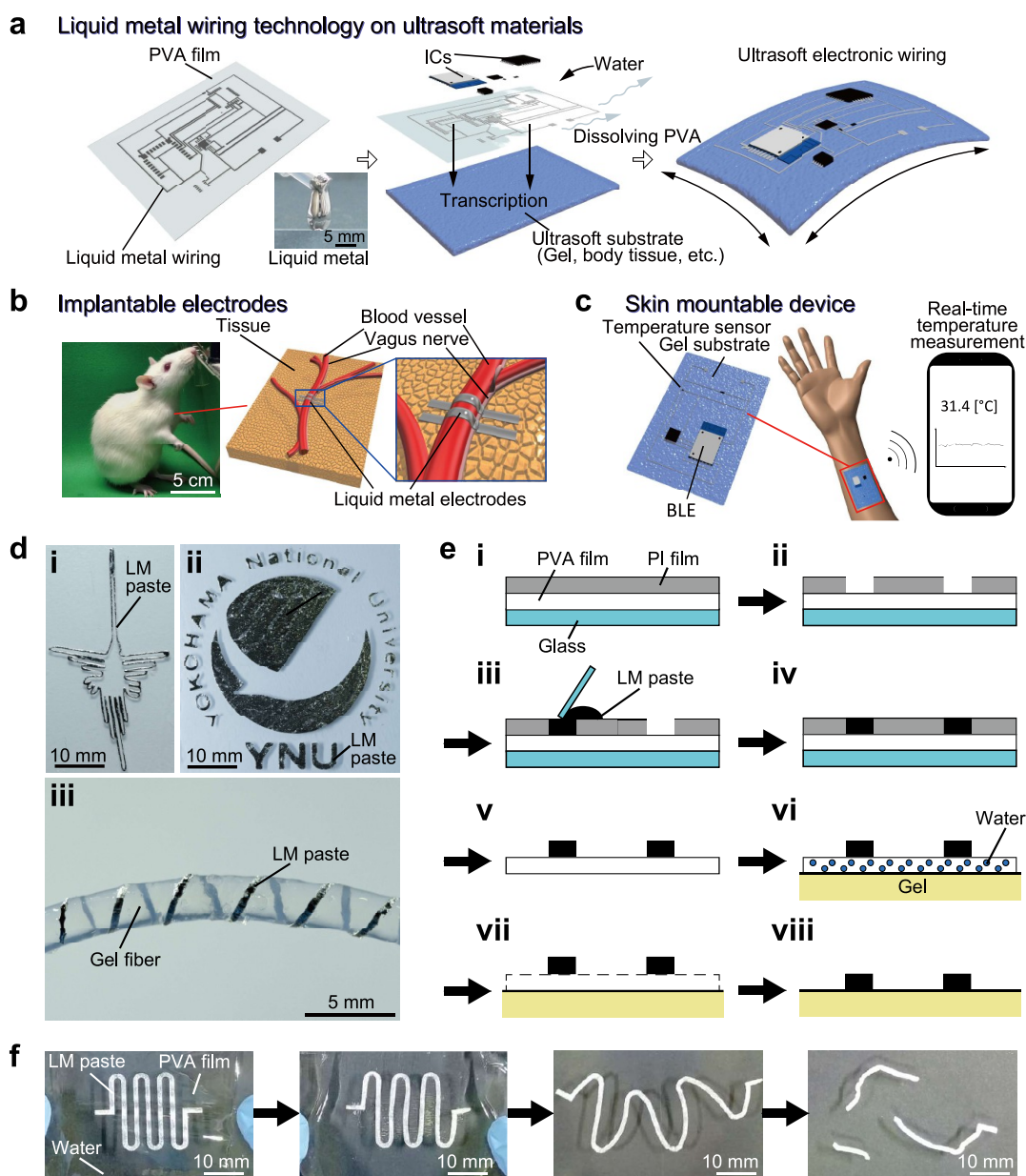


Figure 1. Patterning of Ga-based liquid metal (LM) paste on ultrasoft materials using the polyvinyl alcohol (PVA) lift-off method. (a) Schematics of the patterning process of LM paste composed of Galinstan and Ni powders on soft materials based on the PVA lift-off method. First, screen-printing is used to pattern LM paste on PVA. Second, in some cases, electronic devices are placed on the PVA. Finally, by dissolving the PVA, electric components are implemented on the ultrasoft material, which completes the system. (b) Image of LM paste patterning on biological tissues using the proposed method. (c) Schematic of temperature measurement device fabricated on a gel using the proposed method. (d) Actual photograph of LM paste patterning. (i, ii) Two-dimensional patterns in desired form and (iii) helical patterning on a gel fiber. (e) Fabrication process of LM paste patterning. (f) Photographs showing the disappearance of PVA film patterned with LM paste after the infiltration of water.

Studies on conventional methods for wiring LM have mainly focused on imprinting methods, injection techniques, selective wetting methods, microcontact printing methods, and direct laser patterning.^{19,20} These methods are intended for conventional, flexible, and stretchable substrates such as PDMS. However, it is difficult to apply them to more flexible and softer substrates such as hydrogels, which have poor wettability with LM.

In conventional methods, Ga-based LMs are wired to ultrasoft materials such as gels and biological tissues using a magnet,¹⁰ sintering,²¹ and direct transfer.²² However, these methods can only be used for wiring on a limited substrate or a circuit with a simple structure. For example, in the case of

magnet wiring, a magnet cannot be inserted directly into LM on a substrate with poor wettability or on a surface similar to a closed space.²³ Wiring can be done by moving a magnet across the substrate.¹⁰ This method can only be applied to thin substrates where the magnetic force can penetrate. In the method of direct printing using a brush,²⁴ it is difficult to adjust the wiring width, making it difficult to reduce the size of the circuit. Wiring by sintering using hydrogel mixed with LM particles²¹ and wiring by direct transfer to hydrogel that has good wettability with LM²² require the use of a specific substrate for LM wiring, so the substrate is extremely limited. Therefore, it is not possible to create compact and complex circuits on arbitrary nonplanar substrates using the conven-

tional LM wiring methods on ultrasoft substrates. This issue will be a bottleneck for the realization of conventional devices on ultrasoft materials in the future.

The present study proposes a method for wiring Ga-based LM on ultrasoft materials, biological tissue, and hydrogels treated as substrates based on a polyvinyl alcohol (PVA)-based lift-off process. Based on this method, a sensing system on these materials is also constructed. The LM is first wired on a water-soluble PVA film and then transferred onto ultrasoft materials. This realizes wiring along three-dimensional (3D) substrate shapes such as tissue and 3D wiring on and inside hydrogels. In addition, a system consisting of solid-state electronic elements and LM was developed on the hydrogel to demonstrate the construction of a system on a gel. The findings of this research study are expected to become a cornerstone for the fabrication of systems on ultrasoft substrates.

2. MATERIALS AND METHODS

2.1. Materials and Reagents. PVA, acrylamide, and sodium alginate were obtained from Wako Pure Chemical Industries, Ltd. (Osaka, Japan). Galinstan was obtained from E-Material Ltd. (Tokyo, Japan). Ni powder (3–7 μm) was obtained from Alfa Aesar Co. (Lancashire, UK). *N,N'*-methylenebis acrylamide (BIS), *N,N,N',N'*-tetramethylethylenediamine (TEMED), and ammonium persulfate (APS) were obtained from Nacalai Tesque, Inc. (Kyoto, Japan). Poly(vinylidene fluoride hexafluoropropylene) (PVDF-HFP) was obtained from Arkema (Colombes, France). Ionic liquid (*N*-methyl-*N*-propylpyrrolidiniumbis(trifluoromethanesulfonyl)imide) was obtained from Kanto Chemical Co., Inc. (Tokyo, Japan).

2.2. Basic Principle of LM Paste Wiring. In this study, an LM paste composed of a mixture of Galinstan and Ni powder was wired on the PVA film (Figure 1a), and solid-state electronic elements were mounted if necessary. The PVA film was placed on the substrates (including ultrasoft materials). The electrodes and system circuits were mounted on the substrates by removing the PVA film. This enabled direct wiring (Figure 1b) and system mounting (Figure 1c) on ultrasoft materials such as biological tissues and gels. As shown in Figure 1d_{i,ii}, it is possible to transfer the LM paste to ultrasoft materials in the desired pattern. In addition, LM paste can be wired on the surface of ultrasoft materials with flexible 3D, such as gel fibers (Figure 1d_{iii}).

2.3. Fabrication Method of PVA Film. The PVA used in this study is a fully saponified type with an average degree of polymerization of about 1500–1800. In general, the higher the degree of saponification and the higher the degree of polymerization, the higher the film strength and the lower the water solubility of PVA. In the process of this study, the film strength is important for attaching the adhesive polyimide and peeling off from the glass substrate. However, if the water solubility is low, it is not possible to make a uniform solution, which leads to instability in the properties of the film, so it was necessary to secure a certain degree of solubility while increasing the film strength. Detailed investigations of the degree of polymerization and degree of amendment would be performed in future work. The PVA film was fabricated using the following method. First, 4.5 g of PVA was dissolved in 30 mL of pure water with stirring. The prepared solution was then sonicated for 30 min using an ultrasonic cleaner (US-2R, AS ONE, Osaka, Japan). The solution was then heated with stirring at 200 °C and 1500 revolutions per minute (rpm) for 10 min, and the temperature was then lowered to 120 °C. The desired film was obtained by spin-coating on a glass plate at 1500 rpm for 60 s while maintaining the temperature and then drying the film overnight with exposure to air at approximately 25 °C and from 35 to 40% humidity. The thickness of the PVA film was around 4 μm .

2.4. Fabrication Method of LM Paste. In this study, LM wiring was performed using the screen-printing method. In some cases, screen-printing of LMs such as EGaIn and Galinstan, is difficult

because of their high-surface tension (Figure S1). In particular, in cases of electrodes with large widths such as 1300 μm , an empty area in the electrode emerged as shown in Figure S1. In this study, a maximum line width of 1500 μm is required. Therefore, we developed a LM paste by turning the LM to a paste-like state. The LM paste used in this study has a viscosity of around 189 Pa · s and a yield stress of approximately 204 Pa.¹⁴ Compared to a normal LM, the LM paste provides a more stable connection to solid-state electrical elements due to its higher viscosity. The fabrication method for the LM paste is as follows: The Galinstan was mixed by ultrasonication using an ultrasonicator (SFX 550, BRANSON, Connecticut, US) after dispersing 6 wt % Ni particles (amplitude, 50; time on, 2 s; time off, 4 s; energy, 6 kJ). The LM paste was placed in a styrol case and left overnight with the lid on. In the absence of an acidic environment, the Ni particles stay on the surface of the LM because they are blocked by the oxide film.²⁵ Therefore, in this study, ultrasonication was used to allow the Ni particles to enter into the LM. It is considered that the Ni particles came into contact with the LM and were coated to turn into a paste-like state.

2.5. Wiring Method to Gel. Figure 1e shows the wiring method of the LM paste to gel. First, an adhesive polyimide (PI) film was attached to the spin-coated PVA film on the glass substrate (Figure 1ei). The desired pattern was then fabricated on the PI film using a laser cutter (MD-T1000W, Keyence, Osaka, Japan) (Figure 1eii). The LM paste was coated on the mask of the fabricated PI film, and the pattern of LM paste was fabricated on the PVA film by screen-printing (Figure 1eiii,iv). The PVA film was then peeled off from the glass plate (Figure 1ev) and placed on a substrate such as a hydrogel (Figure 1evi). Water was sprayed (Figure 1evii), and the LM paste was transferred onto the substrate (Figure 1eviii).

As shown in Figure 1f, the solubility of PVA was high, and the transferred PVA dissolved immediately after its contact with the water surface. The LM paste wiring without the substrate disintegrated immediately (Video S1). The 3D images and data of the LM paste wiring were measured using a laser microscope (VK-X250, Keyence, Osaka, Japan).

2.6. Fabrication Method of Gels and Gel Fibers. In this study, acrylamide gel, stretchable acrylamide gel, agarose gel, and ionic gel were used. Acrylamide gel was fabricated by mixing 25 mL of pure water, 2.2 g of acrylamide, 0.025 g of BIS, 60 μL of TEMED, and 0.01 g of APS and pouring the mixture in a mold to cure. Stretchable acrylamide gel was fabricated by mixing 25 mL of pure water, 25 mL of PVA solution, 4.4 g of acrylamide, 0.025 g of BIS, 60 μL of TEMED, and 0.01 g of APS and pouring it in a mold to cure. The agarose gel was fabricated by dissolving 1 g of agarose in 50 mL of phosphate-buffered saline buffer and heating it in a microwave oven at 200 W for 1 min and at 500 W for 1 min after stirring. After confirming the dissolution of the agarose, the solution was poured into a mold and cured. Ionic gel was fabricated by the following procedure: 1.50 g of acetone containing 0.25 g of PVDF-HFP and 1 g of acetone containing 1 g of ionic liquid were stirred. These two solutions were mixed, poured into a mold, and left overnight.

The gel fiber in Figure 1b was fabricated by mixing 6 wt % of AlgNa in pure water and extruding it from the syringe to a 0.15 M CaCl₂ solution by a syringe pump. The injection rate of AlgNa(aq) in the CaCl₂ solution was 0.20 mL/min.

2.7. Vagus Nerve Stimulation Using Animals. Male Sprague–Dawley rats (CrI:CD (SD), body weights: 700–800 g) obtained from Charles River Laboratories Japan, Inc. (Kanagawa, Japan) were housed in plastic cages in a controlled environment (light–dark cycle 12/12 h, temperature 23 \pm 3 °C) with ad libitum access to laboratory basal feed and tap water until the onset of the experimental procedures. All experimental protocols were approved by the Animal Care and Use Committee of the University of Tokyo (no. P21–008). All animals were managed according to the Guidelines for the Care and Use of Laboratory Animals established by the Graduate School of Agriculture and Life Sciences at the University of Tokyo.

Rats (32 weeks of age) were anesthetized with an intraperitoneal injection of urethane and placed in a supine position. The cervical vagus nerve was exposed, and LM paste electrodes or bipolar hook-

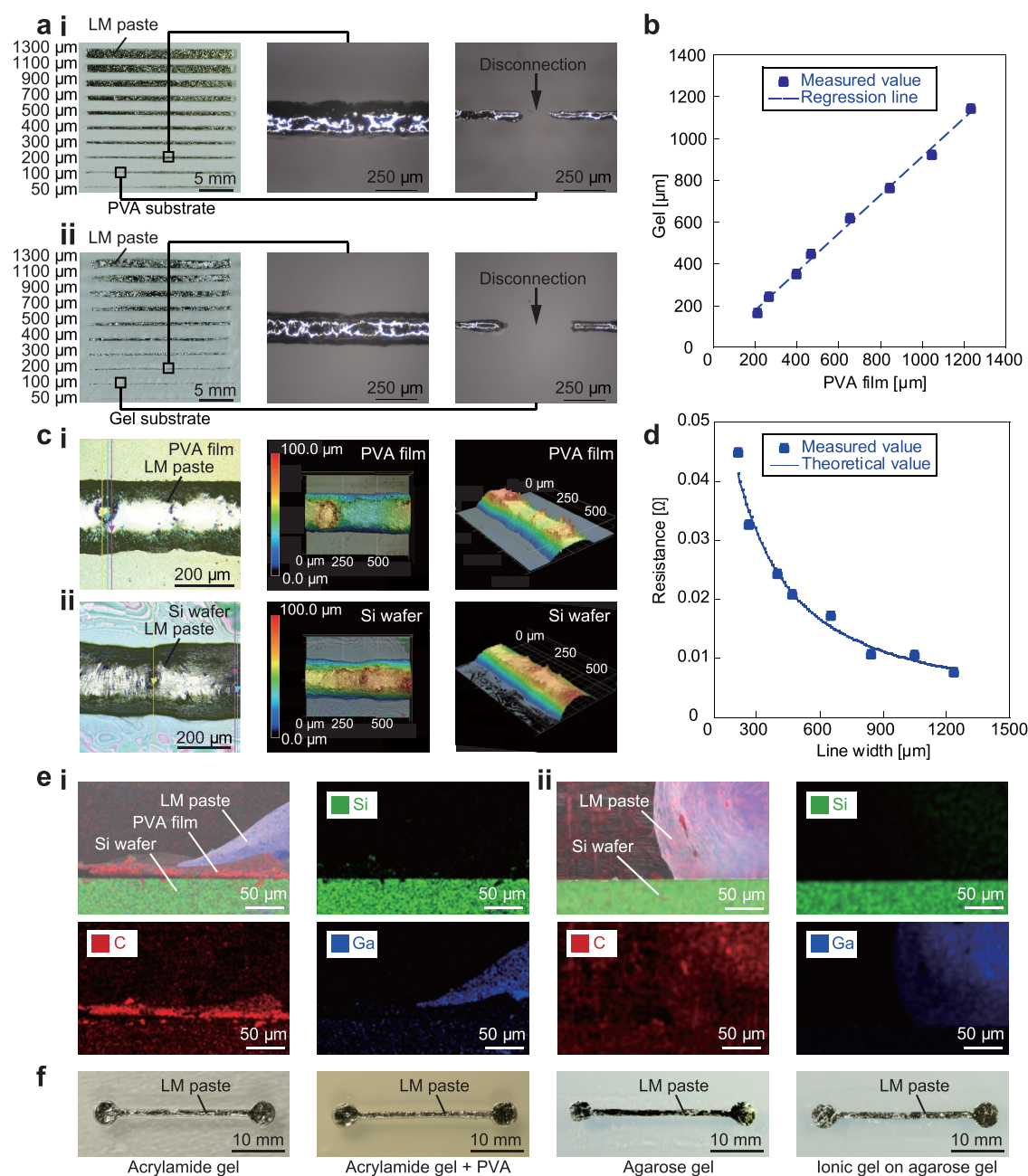


Figure 2. Fundamental characteristics of LM paste patterning on ultrasoft materials. (a) Photographs of LM paste patterns on PVA (i) and hydrogel (ii). The minimum line widths of LM paste on PVA and hydrogel were 212 and 165 μm . (b) Relationships between the line widths of LM paste patterns on PVA film and hydrogel. The LM paste line widths fabricated on PVA could be transferred with almost the same line widths. (c) Images of LM paste patterns on PVA film (i) and silicon (Si) wafer (ii) obtained by laser microscope. (d) Relationship between LM paste line width and resistance value. The resistance value decreased as a function of the line width. (e) Cross-sectional images of LM paste pattern on PVA film (i) and Si wafer after lift-off (ii) using scanning electron microscopy–energy dispersive X-ray spectroscopy. PVA was dissolved by water. (f) LM paste patterns on acrylamide, stretchable acrylamide, agarose, and ionic gels. The method could be used on a variety of gel substrates.

shaped electrodes were attached to the nerve. Needle electrodes were placed on each limb to record the electrocardiogram (ECG, lead II) using transducer amplification equipment (HAS-1, Bio Research Center Co., Ltd., Nagoya, Japan) and the LabChart Pro system (AD Instruments Pty Ltd., New South Wales, Australia). Cervical vagus nerve stimulation (VNS) was then performed with the following settings: 5 V, 10 ms pulse width, and 15 Hz. Consecutive ECG waves were recorded 3 s before and up to 5 s after VNS, and the heart rate (pre-VNS: 3 s average before VNS, post-VNS: 3 s average after the noise and arrhythmia settled 2 s after VNS) were calculated.

2.8. 3D Wiring. Figure S2 shows the fabrication process for the 3D wiring of the LM paste. The LM paste was wired along the dimple

of the gel. The red light-emitting diode (LED) was placed on the LM paste pattern using a die bonder (7200CR, West-Bond Inc., California, US), and the gel was then poured into the dimple and cured. Subsequently, the LM paste was wired on the integrated gel, and the additional green LED was placed again.

2.9. Temperature Measurement Device. A biocompatible agarose gel and ionic gel were used as substrates. Figures S3 and S4 show the fabrication process and circuit diagram, respectively. The voltage between a fixed resistor and a variable resistor (thermistor) (NCP15XH103F03RC (Murata Manufacturing Co., Ltd.)) was detected and converted to temperature by a microcontroller unit (MCU). The converted temperature was transmitted to a smartphone

via a Bluetooth low-energy (BLE) module. The temperature was displayed in real time on the screen. Each element used in the system was placed using a die bonder. The temperature sensing test of the device was performed in an oven.

3. RESULTS AND DISCUSSION

3.1. Fundamental Characteristics of LM Paste Wiring.

Figure 2a shows the wiring state of the LM paste on the PVA film before and after transfer onto the hydrogel. The hydrogel was sufficiently polymerized and stable such that it would not have been dissolved by water during transfer. The LM paste was transferred to the gel without any change in integrity due to its high viscosity and high specific gravity. In addition, the LM paste did not move significantly during the transfer. Hence, the LM paste can be positioned by positioning the PVA film. The wired LM paste did not fall off even when the gel was rotated 180 degrees (Figure S5). This means that the LM paste has sufficient adhesiveness to the gel. The minimum line width on the PVA film was 212 μm . The minimum line width on the gel was 165 μm . However, the viscosity of the LM paste and the wettability of the substrate may affect the patterning resolution, so a detailed investigation of these factors is a subject for future work. As a basic property analysis, a tensile test was conducted using a stretchable acrylamide gel mixed with PVA, confirming that the gel could withstand 71.5% strain (Figure S6). In addition, the wired LM paste remained conductive even after 100 repetitions of 20% strain (Figure S7). In Figure S7, the resistance and its rate of change decreased as the number of times passed, indicating that the gel used as the substrate shrank by drying. Figure 2b shows the relationship between the line width of the LM paste on the PVA film and the line width of the LM paste after it was transferred onto the gel. As the line width on the PVA film increased, the line width on the gel also increased, thus indicating that the line width of the LM paste fabricated on the PVA was directly transferred onto the gel. The correlation coefficient R between the line width on the PVA film and the line width on the gel was 0.998. Figure 2b shows that the line width on the gel is smaller than that on the PVA film for the same LM paste wiring. This is due to the increase in the contact angle, and no loss of the LM paste is considered to have occurred. The height of the LM paste was measured using a laser microscope, and the results are shown in Figure 2c. As a result, the average height of the LM paste wires was approximately 100.5 μm . In addition, the heights were almost constant regardless of the line width. The height of the LM paste increased slightly after transfer compared to before transfer, which is thought to be due to the increase in contact angle. Figure 2d shows the relationship between the line width and resistance at a fixed length (4.712 mm). The resistance value decreased with respect to the line width. The theoretical value was calculated from the resistance in eq 1, and the results of the height are shown in Figure 2c.

$$R = \rho \frac{L}{S} \quad (1)$$

Here, R is the resistance, ρ is the conductivity, L is the length, and S is the cross-sectional area. As shown in Figure 2d, the theoretical and measured resistance values are in agreement. Furthermore, this means that the height measurement shown in Figure 2c is accurate.

The minimum line width that can be fabricated in this study is 165 μm . Benchmarks for related technologies have achieved

85 μm by wiring using a magnet across a gel substrate,¹⁰ approximately 3.3 μm by sintering using hydrogel mixed with LM particles,²¹ and approximately 100 μm by direct transfer to a hydrogel that has good wettability with LM.²² However, these methods require a thin substrate where the magnetic force can reach or a specific substrate, so it is not possible to wire LM on arbitrary nonplanar ultrasoft substrates. In contrast, the LM paste transfer method in this study can be used for wiring on the surface of a thick substrate, such as a body surface, which is difficult to achieve with the existing technologies described above. Additionally, uniform wiring on a textured surface is possible. To fabricate finer lines in the future, it is expected that the LM wiring method on the PVA film will be improved by changing the method from screen-printing to a more precise method such as lithography and by further investigating the properties of the LM paste.

Reports on technologies used to transfer evaporated gold thin film patterns²⁶ or printed silver nanoparticle patterns²⁷ onto substrates using PVA films have been published. These are useful for integration and systemization because they can produce fine lines. In addition, using meander wiring technology, it may be possible to fabricate electrodes that can withstand expansion and contraction. The wiring using LM paste proposed in this study has the advantage where the LM, which is a conductive material, has a lower Young's modulus than that of gel and can therefore be wired without disturbing the deformation of the substrate, even if an ultrasoft substrate such as a gel is used. In addition, a thermal transfer method using fructose²⁸ has been studied. However, this method requires heating to 80 $^{\circ}\text{C}$, and the wiring is upside down during transfer, making it difficult to transfer the system itself to biological tissues. In previous studies, a stretchable conductor was created by applying LM, and an LM pattern with high permeability was achieved.^{29,30} The Young's modulus of the stretchable conductor is 0.1 MPa, which is close to that of human skin. One of the advantages of our study is that it is possible to fabricate ultrasoft electrical wiring by dissolving the substrate with water and conducting LM wiring directly on the biological tissue, which will cause less discomfort when attached to the human body. On the other hand, the long-term stability and air permeability would be low because of the direct patterning of LM.

Figure 2e shows the cross sections of the LM paste wire and the substrate when wiring on the PVA film and when transferring to a silicon wafer (Si wafer). The PVA film between the LM paste and the substrate disappeared when water was sprayed. This indicates that the PVA film was dissolved in water and the LM paste and substrate came into contact. Eventually, the LM paste and substrate became conductive. The wettability of the Si wafer and LM was worse than that of the PVA film because the contact angle was larger than that of the PVA film. In this study, both substrate surfaces were treated with hydrophilic treatments using an excimer lamp. However, the contact angle may increase as a result of water entering between the temporarily formed surface and the LM paste (even momentarily) during the dissolution of PVA. Figure S8 shows a chemical explanation of the phenomena occurring in the transfer process. First, water applied on the PVA film penetrates into the PVA film due to its osmotic pressure. As a water-soluble polymer, PVA has many hydroxy groups in its main chain, which makes it easily soluble in water. (In this case, the oxidized film on the Si wafer also has hydroxy groups, which makes it wettable with water and helps water

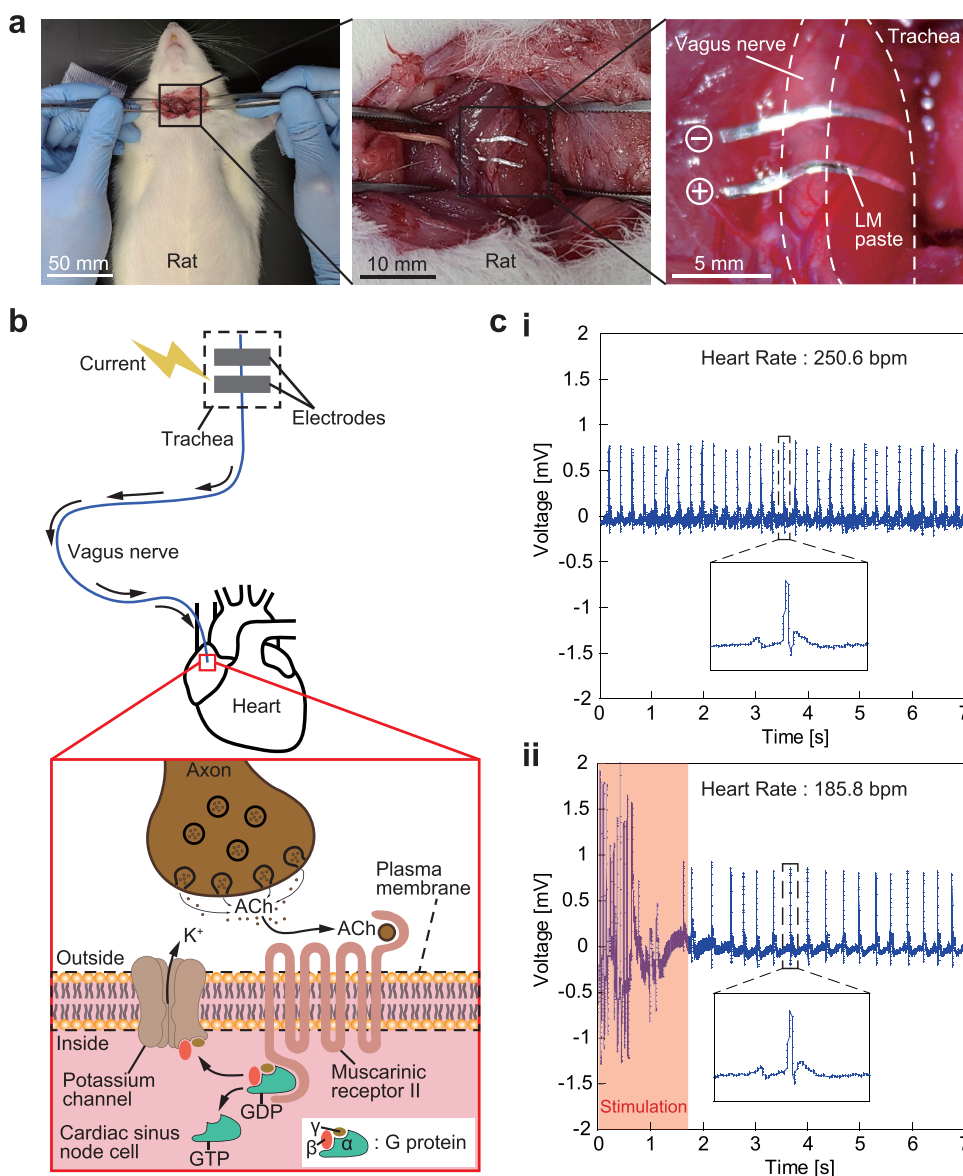


Figure 3. LM paste pattern for vagus nerve stimulation in rats. (a) Depiction of LM paste on the vagus nerve in a rat. (b) Mechanism of heart rate reduction attributed to vagus nerve stimulation. (c) Electrocardiograms before (i) and after (ii) vagus nerve stimulation. The heart rate was decreased by vagus nerve stimulation achieved with the use of the LM paste.

penetrate the PVA film.) The wettability between the LM paste and water was poorer than that between the LM paste and PVA film, resulting in a larger contact angle. Then, the PVA film melted, and the LM paste was transferred onto the Si wafer due to its large specific gravity. Figure S9 shows that the contact angle after the transfer is larger than that before the transfer, and that the contact angle after the transfer is larger than that after the direct screen-printing on the Si wafer. Therefore, it is clear that the wettability between LM paste and water is poorer than that between the LM paste and PVA film. Figure S9a shows that the contact angle hardly changes when screen-printed directly on the Si wafer regardless of the hydrophilic treatment. This indicates that the possibility that the hydrophilic treatment of the Si wafer was lost due to the contact of the PVA film is unrelated to the change in the contact angle. The fact that the contact angle between the LM paste and the Si wafer was almost the same regardless of the hydrophilic treatment is thought to be due to the fact that the oxide film on the Si wafer has hydroxy groups. Figure 2f shows

the transfer of the LM paste wiring onto the acrylamide gel, stretchable acrylamide gel mixed with PVA solution, agarose gel, and ionic gel. LM paste wiring was possible on general gels and hydrogels and was also transferred to PDMS, ECOFLEX, and PI substrates (Figure S10).

3.2. Vagus Nerve Direct Stimulation Using LM Paste Electrodes. As a demonstration of the LM paste wiring technology using the transfer method in this study, we performed cardiac stimulation by direct stimulation of the vagus nerve using LM paste wiring (Figure 3a). As shown in Figure 3b, when the vagus nerve is electrically excited, the excitation is transmitted to the nerve endings through axons, and the neurotransmitter acetylcholine (ACh) is released. ACh binds to the muscarinic receptor II on the cardiac sinus nodal cells and activates G protein-regulated potassium channels via β and γ G proteins. As a result, the sinus nodal cells hyperpolarize, thus leading to the efflux of potassium ions from the intracellular space.

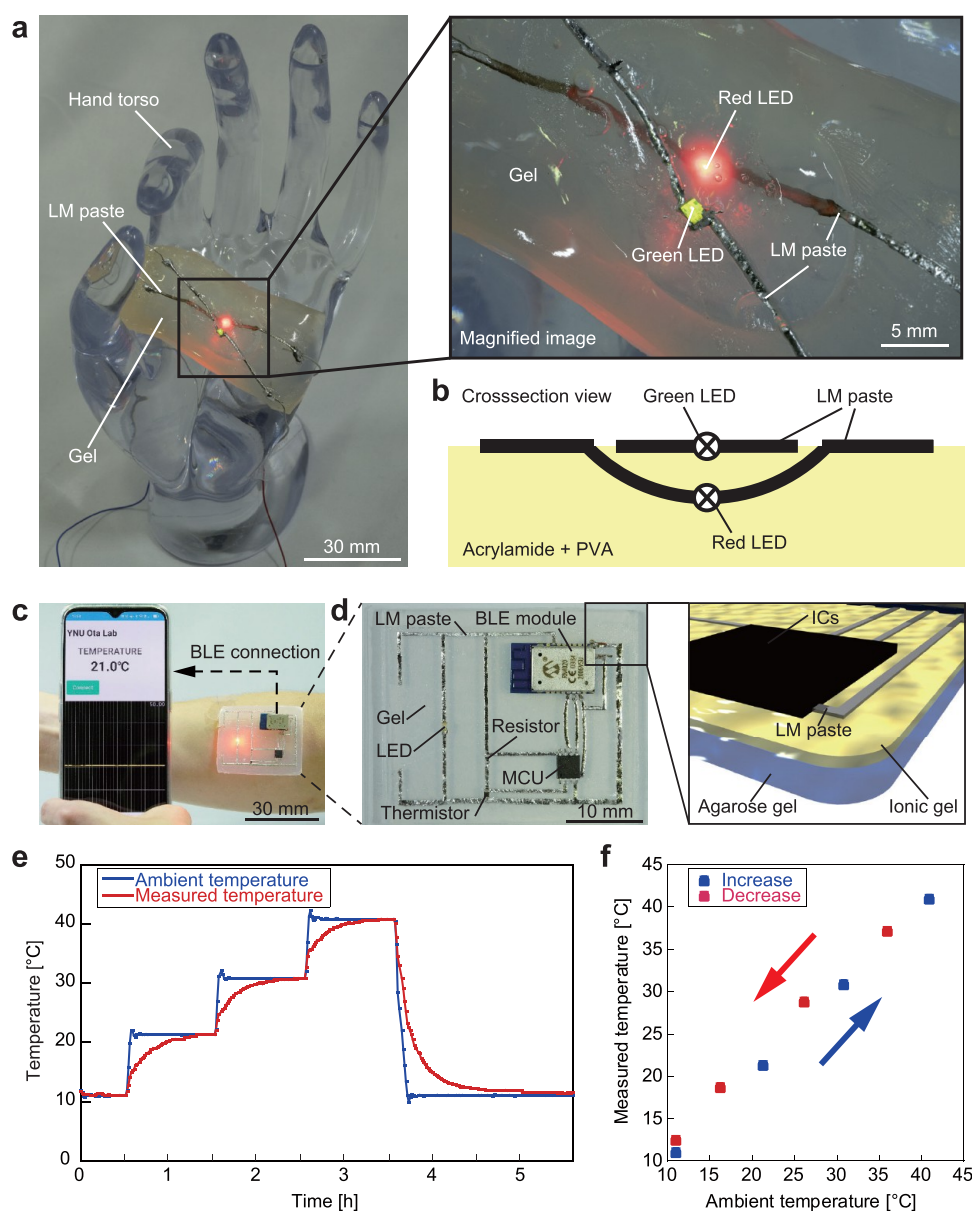


Figure 4. Construction of the system on a gel substrate using LM paste. (a) Construction of the LM paste patterning and lighting of the light-emitting diode on and inside the gel. (b) Cross-sectional image of the circuit structure using LM paste. (c) Temperature measurement device using a gel substrate attached to the arm. The LED lights up when the device works. (d) Top view of the fabricated device and schematic showing the cross-sectional structure of the device. (e) Variation of ambient temperature versus time and device-measured temperature. (f) Relationship between the ambient and measured temperatures of the device.

In fact, the PVA film depicting the LM paste patterning was placed on the vagus nerve exposed by cervical skin incision and connective tissue dissection. Water was then used to dissolve the PVA film so that the LM paste could contact and stimulate the vagus nerve. Finally, a stimulation pulse (5 V, 10 ms pulse width, 15 Hz) was applied between the electrodes (Figure S11). As shown in Figure 3c, the heart rate decreased from 250 bpm before stimulation to 186 bpm after the stimulation.

As a control, the same electrical stimulation was conducted using a hook-shaped electrode (Figure S12). Using a commonly used hook-shaped electrode, the carotid artery and vagus nerve were completely detached from the connective tissue (Figure S12a), the electrode was placed so that the nerve tissue was lifted, and pulsed electrical stimulation was applied (5 V, 10 ms pulse width, and 15 Hz) (Figure S12b). As a result, as shown in Figure S12c, heart rate decreased from 320

to 171 bpm. Electrical stimulation using LM paste was similar to that using a hook-shaped electrode.

The present technique (which uses LM paste) minimized the detachment of the carotid and vagus nerves from the connective tissue and stimulated the vagus nerve without applying stretch stress to the nerve tissue (Figure S12a). In other words, it was possible to implant the electrode without physical stress on the soft tissue. In addition, the use of LM paste made it easy to remove and replace the electrodes because the electrode could be removed by simply wiping the electrode placement area. In this study, the durability of the exposed LM paste pattern was not a challenge because the wiring was designed to be removed. However, when considering long-term use as an implant, it is necessary to improve the durability of the LM paste pattern by sealing the LM paste with the gel. In addition, a previous study reported

that Ni has adverse biological effects on biological tissues.³¹ Ni was used in this study to make the LM into a paste. At the same time, it has been reported that this objective can be achieved with particles such as quartz.³² Therefore, as a future prospect, the LM pastes with other particles could be used to evaluate actual effects on biological tissues.

Previous studies^{33,34} that placed electrodes on the spinal cord tissue and sciatic nerves of rats used PDMS or dimethacrylate-modified polymer perfluoropolyether as substrates. The transfer method in this study has the distinct feature in that the substrate eventually melts and disappears, which makes it more flexible. Another study used LM to fabricate electrode arrays to electrically stimulate biological tissue at the tissue-contacting surface.³⁵ The LM paste electrodes fabricated in this study are easier to connect and more flexible because they adhere to the biological tissue to make contact. The adhesiveness of the LM paste can be considered to be sufficient because vagus nerve stimulation was achieved. It is necessary to investigate this to achieve higher adhesion in the future. A study on the fabrication of conductive gel composites using CNT sheets as *in vivo* electrodes⁸ was proven to be inexpensive and easy to use. However, an alternating current power supply was required. The proposed LM paste can be used with a direct current power supply because the paste is a conductive material.

3.3. 3D Wiring on Hydrogel. The 3D wiring of the LM paste was performed on the hydrogel (Figure 4a). A green LED was placed on the upper side, and a red LED was placed on the lower side. They were connected to the LM paste, as shown in Figure 4b. When a voltage was applied, each LED was lit up. The lower LED was sealed in the gel and wired in such a way that it sank in the gel. Using the gel as an insulating layer between the upper and lower layers, the upper and lower layers were not electrically connected (Figure S13). This experiment proved that electricity can be conducted through the LM paste on the hydrogel. Furthermore, as shown in Figure 4b, it is possible to construct a heterojunction of LM paste and solid-state electronic components on an ultrasoft material such as a hydrogel.

Conventionally, to fabricate 3D LM wiring, the following methods have been used: 3D wiring by introducing LM into 3D channels,^{36–38} 3D wiring with LM by stacking two-dimensional (2D) wiring,³⁹ and direct 3D wiring using dispensers.^{40–42} Although the method of introducing LM into 3D channels fabricated by 3D printers is easy to construct, it is difficult to design the circuit because the channel has to be a single-stroke channel to fabricate fine lines. In the case of the transformation of 2D wiring to 3D, when the wiring is as flexible as PDMS, fine lines can be constructed in 3D with high accuracy by using a lithography process. Regarding 3D direct wiring technology, ultrafine lines can be depicted with a high degree of spatial freedom on solid or rubber substrates. Conversely, in terms of 3D direct wiring on materials that are ultrasoft and have extremely poor LM wettability, such as gels, it is difficult to achieve the desired wiring pattern while maintaining conductivity.⁴³ The method proposed in this study can be used to fabricate 3D wiring even on gel substrates, which are ultrasoft and have low-LM wettability, although the accuracy of the method in this study needs to be improved from the current level of 165 μm . Furthermore, similar to the study of helical wiring on the surface of glass tubes,²³ the helical structure of the wiring (Figure 1d) can also be fabricated using gel fibers, which cannot be easily used as a

substrate. This means that our method can be applied to ultrasoft and low-wettability tubular substrate surfaces. The transferred LM paste and the 3D printed curved surface with a radius of curvature of 600 μm make conformal contact as shown in Figure S14. Conformal interconnection was possible at the board edge with a relatively small radius of curvature. In this experiment, wiring was fabricated using two layers of gel, but it is possible to fabricate more than three gel layers. It is expected that a more multifunctional system can be fabricated in the future.

3.4. Temperature Measurement Device Based on Hydrogel Substrate. Figure 4c shows the developed device worn on the arm. The LED on the device was lit to confirm that the device was working. In addition, the measured temperature and temperature transitions are displayed in a graph on the smartphone. The device adhered to the arm without any adhesive and functioned by sticking it to the arm, even when the arm was rotated up to 90 degrees along its axis. This is due to the large adhesive area of the gel when it adheres to the skin and generates a relatively high-adhesion force for the thickness of the device. This adhesion is expected to be further improved by reducing the thickness of the gel. Figure 4d shows the device. The temperature measurement circuit was constructed by placing an ionic gel on top of the agarose gel and wiring LM paste on top of the ionic gel. The agarose gel had a narrow potential window because water was also included. Therefore, in this study, the ion gel was coated on top of the agarose gel, and the LM paste was wired on top of the ion gel (Figure 4d). This device used a thermistor to detect the difference in voltage depending on the temperature. Specifically, voltage differences were converted to temperature by the MCU, and the converted temperature was transmitted to the smartphone via the BLE module. Figure 4e,f shows the temperature changes on the device when the ambient temperature increases or decreases. The temperature measured by the device is associated with the ambient temperature. In addition, there was almost no hysteresis. This indicates that the connection between the LM paste wiring and solid-state electric elements on the gel was stable, and the robustness of the system was high. The conventional substrate for the connection between the LM and the circuit elements for making advanced smart devices was based on a flexible polymer or rubber substrate such as PI, polyethylene naphthalate (PEN), polyethylene terephthalate (PET), parlylene, PDMS, Ecoflex, and polyurethane (PU).^{39,44,45} However, in this study, softer gel substrates were used to achieve this connection on the substrate. In this study, we proposed new circuit substrates with LMs as electrodes.

As conductive materials have similar mechanical properties to those of gels, studies have been conducted on conductive hydrogels using CNTs, PEDOT:PSS, and polyaniline (PANI).^{8,46–49} The resistance change as a function of strain is usually large because these materials often use the percolation effect, and the conductivity is less than $1.0 \times 10^5 \text{ Sm}^{-1}$. Therefore, they are useful as sensor elements such as pressure and strain sensors. In contrast, the conductivity of LM paste (6 wt %) is $2.92 \times 10^6 \pm 0.68 \times 10^6 \text{ Sm}^{-1}$ ($n = 3$), which is suitable for wiring when fabricating systems because it does not utilize the percolation effect. Based on the above listings, a system that employs ultrasoft substrates such as gels could be realized in this study using a conductive liquid material. Replacing the temperature measurement system realized by the transfer method in this study with other systems and creating a

system that measures skin temperature by wiring the LM paste directly to the skin as a substrate are future prospects. The electrodes to be fabricated by the transfer method in this study can be expected to have applications in the biomedical field, such as diagnostic devices.

4. CONCLUSIONS

This study proposed a method of transferring LM paste onto ultrasoft materials such as hydrogels using PVA film and presented the construction of a complete system. LM paste patterns fabricated on PVA films adhered to the ultrasoft substrate along surface irregularities and were transferred without destruction following the dissolution of the PVA films in water. The minimum wire width of the LM paste was approximately 165 μm , and the LM paste pattern on PVA was transferred on the hydrogel with the same wire width. Vagus nerve stimulation using LM paste wiring successfully applied this transfer method to biological tissues. In addition to the helical wiring of LM paste on the surfaces of ultrasoft gel fibers, the transfer method also enabled the wiring of 3D intersecting structures on hydrogels. By using the gel as an insulating layer, no electrical crosstalk occurred and multiple independent wires of LM paste were fabricated. Furthermore, the transfer of the temperature measurement system constructed on the PVA film onto the gel was demonstrated. The connection between the solid-state electronic device and the LM paste was stable, which maintained the functionality of the system on the gel. Using the 3D interconnection technique described above, it may be possible to integrate multiple systems in a single device across an insulating layer of gels. This fundamental fabrication and system integration technique may be applied to wearable devices with higher flexibility as well as implantable devices and gel actuators that can measure the health status of the body.

■ ASSOCIATED CONTENT

SI Supporting Information

The Supporting Information is available free of charge at <https://pubs.acs.org/doi/10.1021/acsami.1c20628>.

LM paste screen-printing according to the Ni particle concentration; fabrication process of 3D structure of LM paste on and inside the gel; fabrication process of the temperature measurement device on gels; circuit diagram of the temperature measurement system; photographs of LM paste patterns transferred onto hard or rubber substrates; pulse voltage waveform applied to the vagus nerve of a rat; vagus nerve stimulation in a rat using a hook-shaped electrode; independent lighting of each LED in the LM paste 3D structure (PDF)

Disappearance of PVA film patterned with LM paste by water (MP4)

■ AUTHOR INFORMATION

Corresponding Authors

Ohmi Fuchiwaki – Department of Mechanical Engineering and Graduate School of System Integration, Yokohama National University, Yokohama, Kanagawa 240-8501, Japan; Phone: +81-45-339-4324; Email: fuchiwaki-ohmi-xk@ynu.ac.jp

Hiroki Ota – Department of Mechanical Engineering and Graduate School of System Integration, Yokohama National

University, Yokohama, Kanagawa 240-8501, Japan; orcid.org/0000-0002-3702-6357; Phone: +81-45-339-4334; Email: ota-hiroki-xm@ynu.ac.jp

Authors

Koki Murakami – Department of Mechanical Engineering, Yokohama National University, Yokohama, Kanagawa 240-8501, Japan

Ryota Tochinai – Graduate School of Agricultural and Life Sciences, The University of Tokyo, Tokyo 113-8657, Japan

Daiki Tachibana – Department of Mechanical Engineering, Yokohama National University, Yokohama, Kanagawa 240-8501, Japan

Yuji Isano – Department of Mechanical Engineering, Yokohama National University, Yokohama, Kanagawa 240-8501, Japan

Ryosuke Matsuda – Department of Mechanical Engineering, Yokohama National University, Yokohama, Kanagawa 240-8501, Japan

Fumika Nakamura – Department of Mechanical Engineering, Yokohama National University, Yokohama, Kanagawa 240-8501, Japan

Yuta Kurotaki – Department of Mechanical Engineering, Yokohama National University, Yokohama, Kanagawa 240-8501, Japan

Yutaka Isoda – Graduate School of System Integration, Yokohama National University, Yokohama, Kanagawa 240-8501, Japan

Monami Yamane – Department of Chemistry and Life Science, Yokohama National University, Yokohama, Kanagawa 240-8501, Japan

Yuya Sugita – Department of Chemistry and Life Science, Yokohama National University, Yokohama, Kanagawa 240-8501, Japan

Junji Fukuda – Graduate School of Engineering, Yokohama National University, Yokohama, Kanagawa 240-8501, Japan

Kazuhide Ueno – Graduate School of Engineering, Yokohama National University, Yokohama, Kanagawa 240-8501, Japan; orcid.org/0000-0002-4684-5717

Norihisa Miki – Department of Mechanical Engineering, Keio University, Yokohama, Kanagawa 223-8522, Japan

Complete contact information is available at: <https://pubs.acs.org/10.1021/acsami.1c20628>

Author Contributions

K.M. collected all data and led all experiments. R.T. helped conduct the animal experiment. D.T. helped fabricate the stretchable acrylamide gel. Y. Isano helped make patterned masks. R.M. helped make acrylic resin molds. F.N. helped make the liquid metal paste and created the temperature measurement system. Y.K. created the real-time temperature display application. Y. Isoda helped record data on electrical stimulation. M.Y. and J.F. helped fabricate the agarose gel. Y.S. helped measure the data using the laser microscope. K.U. helped fabricate the ionic gel. N.M. helped investigate the properties of gels. O.F. and H.O. guided the research. K.M., O.F., and H.O. wrote the paper.

Notes

The authors declare no competing financial interest.

ACKNOWLEDGMENTS

This work was supported by the PRESTO/Japanese Science and Technology Agency (JST) (grant no. JPMJPR18J2), and JST CREST (grant no. JP19209665). H.O. acknowledges support from a Grant-in-Aid for Challenging Exploratory Research and a Grant-in-Aid for Scientific Research (A) provided by the Japanese Society for the Promotion of Science.

REFERENCES

- (1) Areir, M.; Xu, Y.; Harrison, D.; Fyson, J. A Study of 3D Printed Flexible Supercapacitors onto Silicone Rubber Substrates. *J. Mater. Sci.: Mater. Electron.* **2017**, *28*, 18254–18261.
- (2) Ji, B.; Xie, Z.; Hong, W.; Jiang, C.; Guo, Z.; Wang, L.; Wang, X.; Yang, B.; Liu, J. Stretchable Parylene-C Electrodes Enabled by Serpentine Structures on Arbitrary Elastomers by Silicone Rubber Adhesive. *J. Mater.* **2020**, *6*, 330–338.
- (3) Huang, L.; Wang, H.; Wu, P.; Huang, W.; Gao, W.; Fang, F.; Cai, N.; Chen, R.; Zhu, Z. Wearable Flexible Strain Sensor Based on Three-Dimensional Wavy Laser-Induced Graphene and Silicone Rubber. *Sensors* **2020**, *20*, 1–14.
- (4) Li, J.; Guo, C.; Wang, Z.; Gao, K.; Shi, X.; Liu, J. Electrical Stimulation towards Melanoma Therapy via Liquid Metal Printed Electronics on Skin. *Clin. Transl. Med.* **2016**, *5*, 21.
- (5) Liu, Y.; Liu, J.; Chen, S.; Lei, T.; Kim, Y.; Niu, S.; Wang, H.; Wang, X.; Foudeh, A. M.; Tok, J. B. H.; Bao, Z. Soft and Elastic Hydrogel-Based Microelectronics for Localized Low-Voltage Neuromodulation. *Nat. Biomed. Eng.* **2019**, *3*, 58–68.
- (6) Liu, J.; Zheng, H.; Poh, P.; Machens, H.-G.; Schilling, A. Hydrogels for Engineering of Perfusable Vascular Networks. *Int. J. Mol. Sci.* **2015**, *16*, 15997–16016.
- (7) Jeon, M.; Cho, J.; Kim, Y. K.; Jung, D.; Yoon, E. S.; Shin, S.; Cho, I. J. Partially Flexible MEMS Neural Probe Composed of Polyimide and Sucrose Gel for Reducing Brain Damage during and after Implantation. *J. Micromech. Microeng.* **2014**, *24*, No. 025010.
- (8) Sekitani, T.; Yokota, T.; Kuribara, K.; Kaltenbrunner, M.; Fukushima, T.; Inoue, Y.; Sekino, M.; Isoyama, T.; Abe, Y.; Onodera, H.; Someya, T. Ultraflexible Organic Amplifier with Biocompatible Gel Electrodes. *Nat. Commun.* **2016**, *7*, 1.
- (9) Ge, G.; Zhang, Y.; Shao, J.; Wang, W.; Si, W.; Huang, W.; Dong, X. Stretchable, Transparent, and Self-Patterned Hydrogel-Based Pressure Sensor for Human Motions Detection. *Adv. Funct. Mater.* **2018**, *28*, 1802576.
- (10) Xu, C.; Ma, B.; Yuan, S.; Zhao, C.; Liu, H. High-Resolution Patterning of Liquid Metal on Hydrogel for Flexible, Stretchable, and Self-Healing Electronics. *Adv. Electron. Mater.* **2020**, *6*, 1900721.
- (11) Huang, S.; Feng, C.; Mayes, E. L. H.; Yao, B.; He, Z.; Asadi, S.; Alan, T.; Yang, J. In Situ Synthesis of Silver Nanowire Gel and Its Super-Elastic Composite Foams. *Nanoscale* **2020**, *12*, 19861–19869.
- (12) Heo, D. N.; Lee, S. J.; Timsina, R.; Qiu, X.; Castro, N. J.; Zhang, L. G. Development of 3D Printable Conductive Hydrogel with Crystallized PEDOT:PSS for Neural Tissue Engineering. *Mater. Sci. Eng. C* **2019**, *99*, 582–590.
- (13) Jintoku, H.; Matsuzawa, Y.; Yoshida, M. Light-Induced Fabrication of Patterned Conductive Nanocarbon Films for Flexible Electrode. *ACS Appl. Nano Mater.* **2020**, *3*, 8866–8874.
- (14) Daalkhajjav, U.; Yirmibesoglu, O. D.; Walker, S.; Mengüç, Y. Rheological Modification of Liquid Metal for Additive Manufacturing of Stretchable Electronics. *Adv. Mater. Technol.* **2018**, *3*, 1700351.
- (15) Niiyama, R.; Yao, L.; Ishii, H. Weight and Volume Changing Device with Liquid Metal Transducer. *TEI 2014 - 8th Int. Conf. Tangible, Embed. Embodied Interact. Proc.*; 2014, C, 49–52.
- (16) Kozaki, T.; Saito, S.; Otsuki, Y.; Matsuda, R.; Isoda, Y.; Endo, T.; Nakamura, F.; Araki, T.; Furukawa, T.; Maruo, S.; Watanabe, M.; Ueno, K.; Ota, H. Liquid-State Optoelectronics Using Liquid Metal. *Adv. Electron. Mater.* **2020**, *6*, 1–7.
- (17) Gao, Y.; Ota, H.; Schaler, E. W.; Chen, K.; Zhao, A.; Gao, W.; Fahad, H. M.; Leng, Y.; Zheng, A.; Xiong, F.; Zhang, C.; Tai, L. C.; Zhao, P.; Fearing, R. S.; Javey, A. Wearable Microfluidic Diaphragm Pressure Sensor for Health and Tactile Touch Monitoring. *Adv. Mater.* **2017**, *29*, 1701985.
- (18) Takaya, M.; Matsuda, R.; Inamori, G.; Kamoto, U.; Isoda, Y.; Tachibana, D.; Nakamura, F.; Fuchiwaki, O.; Okubo, Y.; Ota, H. Transformable Electrocardiograph Using Robust Liquid-Solid Heteroconnector. *ACS Sensors* **2021**, *6*, 212–219.
- (19) Park, Y. G.; Lee, G. Y.; Jang, J.; Yun, S. M.; Kim, E.; Park, J. U. Liquid Metal-Based Soft Electronics for Wearable Healthcare. *Adv. Healthcare Mater.* **2021**, *10*, No. e2002280.
- (20) Cole, T.; Khoshmanesh, K.; Tang, S.-Y. Liquid Metal Enabled Biodevices. *Adv. Intell. Syst.* **2021**, *3*, 2000275.
- (21) Park, J. E.; Kang, H. S.; Baek, J.; Park, T. H.; Oh, S.; Lee, H.; Koo, M.; Park, C. Rewritable, Printable Conducting Liquid Metal Hydrogel. *ACS Nano* **2019**, *13*, 9122–9130.
- (22) Park, J. E.; Kang, H. S.; Koo, M.; Park, C. Autonomous Surface Reconciliation of a Liquid-Metal Conductor Micropatterned on a Deformable Hydrogel. *Adv. Mater.* **2020**, *32*, No. e2002178.
- (23) Ma, B.; Xu, C.; Chi, J.; Chen, J.; Zhao, C.; Liu, H. A Versatile Approach for Direct Patterning of Liquid Metal Using Magnetic Field. *Adv. Funct. Mater.* **2019**, *29*, 1901370.
- (24) Wang, X.; Fan, L.; Zhang, J.; Sun, X.; Chang, H.; Yuan, B.; Guo, R.; Duan, M.; Liu, J. Printed Conformable Liquid Metal E-Skin-Enabled Spatiotemporally Controlled Bioelectromagnetics for Wireless Multisite Tumor Therapy. *Adv. Funct. Mater.* **2019**, *29*, 1907063.
- (25) Carle, F.; Bai, K.; Casara, J.; Vanderlick, K.; Brown, E. Development of Magnetic Liquid Metal Suspensions for Magneto-hydrodynamics. *Phys. Rev. Fluids* **2017**, *2*, 013301.
- (26) Schaper, C. D. Patterned Transfer of Metallic Thin Film Nanostructures by Water-Soluble Polymer Templates. *Nano Lett.* **2003**, *3*, 1305–1309.
- (27) Saada, G.; Layani, M.; Chernevovsky, A.; Magdassi, S. Hydroprinting Conductive Patterns onto 3D Structures. *Adv. Mater. Technol.* **2017**, *2*, 1–6.
- (28) Guo, R.; Sun, X.; Yuan, B.; Wang, H.; Liu, J. Magnetic Liquid Metal (Fe-EGaIn) Based Multifunctional Electronics for Remote Self-Healing Materials, Degradable Electronics, and Thermal Transfer Printing. *Adv. Sci.* **2019**, *6*, 1901478.
- (29) Zhuang, Q.; Ma, Z.; Gao, Y.; Zhang, Y.; Wang, S.; Lu, X.; Hu, H.; Cheung, C.; Huang, Q.; Zheng, Z. Liquid-Metal-Superlyophilic and Conductivity-Strain-Enhancing Scaffold for Permeable Superelastic Conductors. *Adv. Funct. Mater.* **2021**, 2105587.
- (30) Ma, Z.; Huang, Q.; Xu, Q.; Zhuang, Q.; Zhao, X.; Yang, Y.; Qiu, H.; Yang, Z.; Wang, C.; Chai, Y.; Zheng, Z. Permeable Superelastic Liquid-Metal Fibre Mat Enables Biocompatible and Monolithic Stretchable Electronics. *Nat. Mater.* **2021**, *20*, 859–868.
- (31) Wataha, J. C.; O'Dell, N. L.; Singh, B. B.; Ghazi, M.; Whitford, G. M.; Lockwood, P. E. Relating Nickel-Induced Tissue Inflammation to Nickel Release in Vivo. *J. Biomed. Mater. Res.* **2001**, *58*, 537–544.
- (32) Chang, H.; Zhang, P.; Guo, R.; Cui, Y.; Hou, Y.; Sun, Z.; Rao, W. Recoverable Liquid Metal Paste with Reversible Rheological Characteristic for Electronics Printing. *ACS Appl. Mater. Interfaces* **2020**, *12*, 14125–14135.
- (33) Green, R. Elastic and Conductive Hydrogel Electrodes. *Nat. Biomed. Eng.* **2019**, *3*, 9–10.
- (34) Mineev, I. R.; Musienko, P.; Hirsch, A.; Barraud, Q.; Wenger, N.; Morand, E. M.; Gandar, J.; Capogrosso, M.; Milekovic, T.; Asboth, L.; Torres, R. F.; Vachicouras, N.; Liu, Q.; Pavlova, N.; Duis, S.; Larmagnac, A.; Vörös, J.; Micera, S.; Suo, Z.; Courtine, G.; Lacour, S. P. Electronic Dura Mater for Long-Term Multimodal Neural Interfaces. *Science* **2015**, *347*, 159–163.
- (35) David, R.; Miki, N. Liquid Metal Electrodes Micro-Array for Electrical Stimulation via Direct Contact. *Proc. IEEE Int. Conf. Micro Electro Mech. Syst.* **2018**, 2018, 373–375.
- (36) Ota, H.; Emaminejad, S.; Gao, Y.; Zhao, A.; Wu, E.; Challa, S.; Chen, K.; Fahad, H. M.; Jha, A. K.; Kiriya, D.; Gao, W.; Shiraki, H.; Morioka, K.; Ferguson, A. R.; Healy, K. E.; Davis, R. W.; Javey, A. Application of 3D Printing for Smart Objects with Embedded Electronic Sensors and Systems. *Adv. Mater. Technol.* **2016**, *1*, 1600013.

(37) Matsubara, K.; Tachibana, D.; Matsuda, R.; Onoe, H.; Fuchiwaki, O.; Ota, H. Hydrogel Actuator with a Built-In Stimulator Using Liquid Metal for Local Control. *Adv. Intell. Syst.* **2020**, 2000008.

(38) Wu, S. Y.; Yang, C.; Hsu, W.; Lin, L. 3D-Printed Microelectronics for Integrated Circuitry and Passive Wireless Sensors. *Microsyst. Nanoeng.* **2015**, 1, 1–9.

(39) Kim, M. G.; Kim, C.; Alrowais, H.; Brand, O. Multiscale and Uniform Liquid Metal Thin-Film Patterning Based on Soft Lithography for 3D Heterogeneous Integrated Soft Microsystems: Additive Stamping and Subtractive Reverse Stamping. *Adv. Mater. Technol.* **2018**, 3, 1–10.

(40) Ladd, C.; So, J. H.; Muth, J.; Dickey, M. D. 3D Printing of Free Standing Liquid Metal Microstructures. *Adv. Mater.* **2013**, 25, 5081–5085.

(41) Park, Y. G.; An, H. S.; Kim, J. Y.; Park, J. U. High-Resolution, Reconfigurable Printing of Liquid Metals with Three-Dimensional Structures. *Sci. Adv.* **2019**, 5, No. eaaw2844.

(42) Park, Y. G.; Min, H.; Kim, H.; Zhexembekova, A.; Lee, C. Y.; Park, J. U. Three-Dimensional, High-Resolution Printing of Carbon Nanotube/Liquid Metal Composites with Mechanical and Electrical Reinforcement. *Nano Lett.* **2019**, 19, 4866–4872.

(43) Yu, Y.; Liu, F.; Zhang, R.; Liu, J. Suspension 3D Printing of Liquid Metal into Self-Healing Hydrogel. *Adv. Mater. Technol.* **2017**, 2, 1700173.

(44) Wang, Q.; Yu, Y.; Yang, J.; Liu, J. Fast Fabrication of Flexible Functional Circuits Based on Liquid Metal Dual-Trans Printing. *Adv. Mater.* **2015**, 27, 7109–7116.

(45) Jeong, S. H.; Hjort, K.; Wu, Z. Tape Transfer Atomization Patterning of Liquid Alloys for Microfluidic Stretchable Wireless Power Transfer. *Sci. Rep.* **2015**, 5, 8419.

(46) Ahadian, S.; Ramón-Azcón, J.; Estili, M.; Liang, X.; Ostrovidov, S.; Shiku, H.; Ramalingam, M.; Nakajima, K.; Sakka, Y.; Bae, H.; Matsue, T.; Khademhosseini, A. Hybrid Hydrogels Containing Vertically Aligned Carbon Nanotubes with Anisotropic Electrical Conductivity for Muscle Myofiber Fabrication. *Sci. Rep.* **2014**, 4, 4271.

(47) Feig, V. R.; Tran, H.; Lee, M.; Bao, Z. Mechanically Tunable Conductive Interpenetrating Network Hydrogels That Mimic the Elastic Moduli of Biological Tissue. *Nat. Commun.* **2018**, 9, 2740.

(48) Hu, C.; Zhang, Y.; Wang, X.; Xing, L.; Shi, L.; Ran, R. Stable, Strain-Sensitive Conductive Hydrogel with Antifreezing Capability, Remoldability, and Reusability. *ACS Appl. Mater. Interfaces* **2018**, 10, 44000–44010.

(49) Teo, M. Y.; Ravichandran, N.; Kim, N.; Kee, S.; Stuart, L.; Aw, K. C.; Stringer, J. Direct Patterning of Highly Conductive PEDOT:PSS/Ionic Liquid Hydrogel via Microreactive Inkjet Printing. *ACS Appl. Mater. Interfaces* **2019**, 11, 37069–37076.

**HAZARD AWARENESS
REDUCES LAB INCIDENTS**

**ACS Essentials of
Lab Safety for
General Chemistry**

A new course from the
American Chemical Society

ACS Institute
Learn. Develop. Excel.

EXPLORE
ORGANIZATIONAL
SALES
solutions.acs.org/essentialsoflabsafety

REGISTER FOR
INDIVIDUAL ACCESS
institute.acs.org/courses/essentials-lab-safety.html

Supplementary Information

Direct wiring of liquid metal on ultrasoft substrate using a polyvinyl alcohol lift-off method

Koki Murakami ^a, Ryota Tochinai ^b, Daiki Tachibana ^a, Yuji Isano ^a, Ryosuke Matsuda ^a, Fumika Nakamura ^a, Yuta Kurotaki ^a, Yutaka Isoda ^c, Monami Yamane ^d, Yuya Sugita ^d, Junji Fukuda ^e, Kazuhide Ueno ^e, Norihisa Miki ^f, Ohmi Fuchiwaki ^{a,c,}, Hiroki Ota ^{a,c,*}*

^aDepartment of Mechanical Engineering, Yokohama National University, 79-5, Tokiwadai, Hodogaya-ku, Yokohama, Kanagawa 240-8501, Japan

^bGraduate School of Agricultural and Life Sciences, The University of Tokyo, 1-1-1, Yayoi, Bunkyo-ku, Tokyo 113-8657, Japan

^cGraduate School of System Integration, Yokohama National University, 79-5, Tokiwadai, Hodogaya-ku, Yokohama, Kanagawa 240-8501, Japan

^dDepartment of Chemistry and Life Science, Yokohama National University, 79-5 Tokiwadai, Hodogaya-ku, Yokohama, Kanagawa, 240-8501, Japan

^eGraduate School of Engineering, Yokohama National University, 79-5 Tokiwadai, Hodogaya-ku, Yokohama, Kanagawa, 240-8501, Japan

^fDepartment of Mechanical Engineering, Keio University, 3-14-1, Hiyoshi, Kohoku-ku, Yokohama, Kanagawa 223-8522, Japan

*Corresponding author:

Professor Hiroki Ota

E-mail: ota-hiroki-xm@ynu.ac.jp; Tel.:+81-45-339-4330

Professor Ohmi Fuchiwaki

E-mail: fuchiwaki-ohmmi-xk@ynu.ac.jp; Tel.:+81-45-339-4324

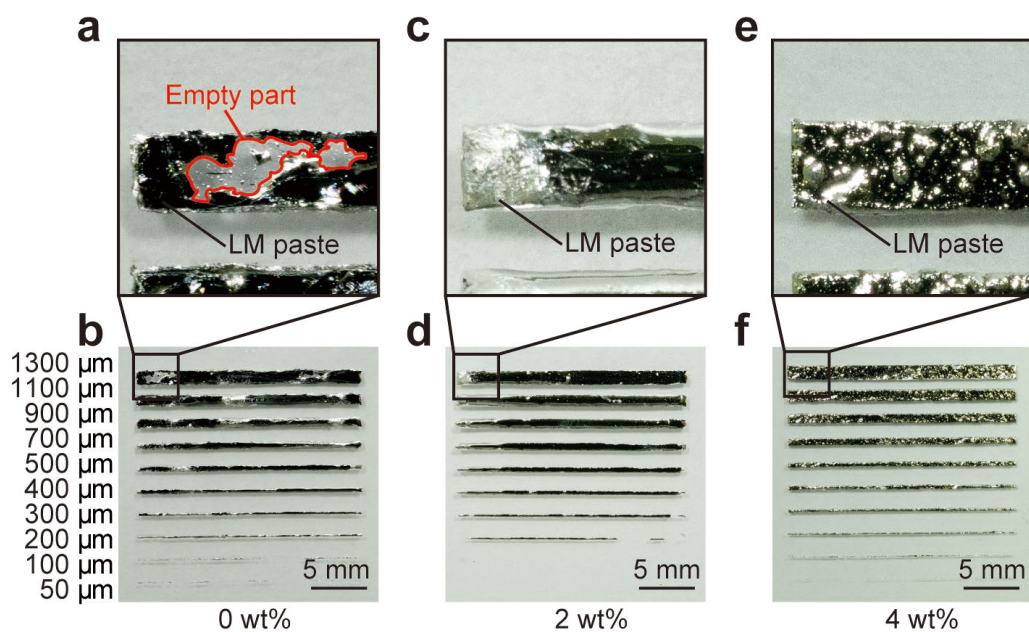


Figure S1. Liquid metal (LM) paste screen-printing according to the Ni particle concentration (a, b) 0 wt%. (c, d) 2 wt%. (e, f) 4 wt%. (a, c, e) When thick electrodes were fabricated, empty parts were formed in the liquid metal without Ni particles because of the low wettability of the gel to liquid metal.

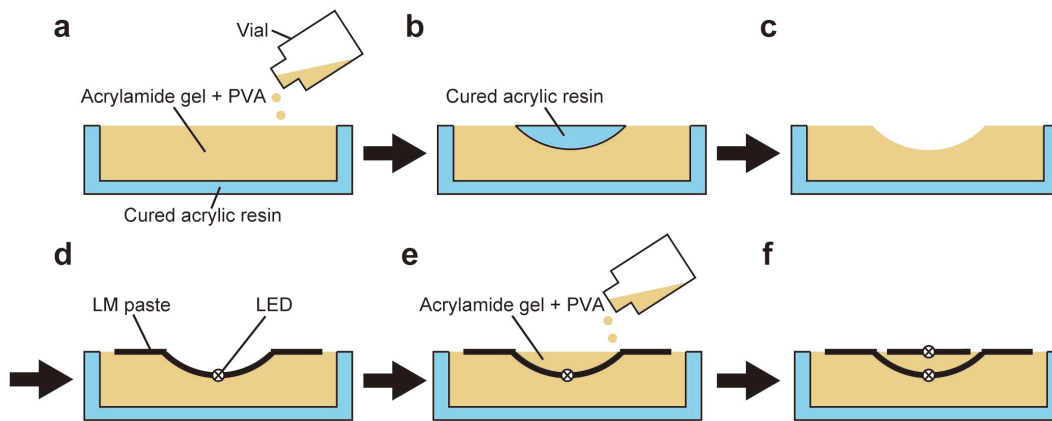


Figure S2. Fabrication process of three-dimensional (3D) structure of LM paste on and inside the gel. (a) Mixture of acrylamide gel and polyvinyl alcohol (PVA) is poured on acrylic resin. (b) Mold of the 3D printed acrylic resin is placed on the gel. (c) Formation of a concave structure. (d) LM paste is patterned by the developed method based on PVA lift-off process and electric components are mounted on the gel. (e) New mixture of acrylamide gel and PVA is poured on the concave part. (f) LM paste is patterned by the developed method based on the PVA lift-off process and electric components are mounted on the gel.

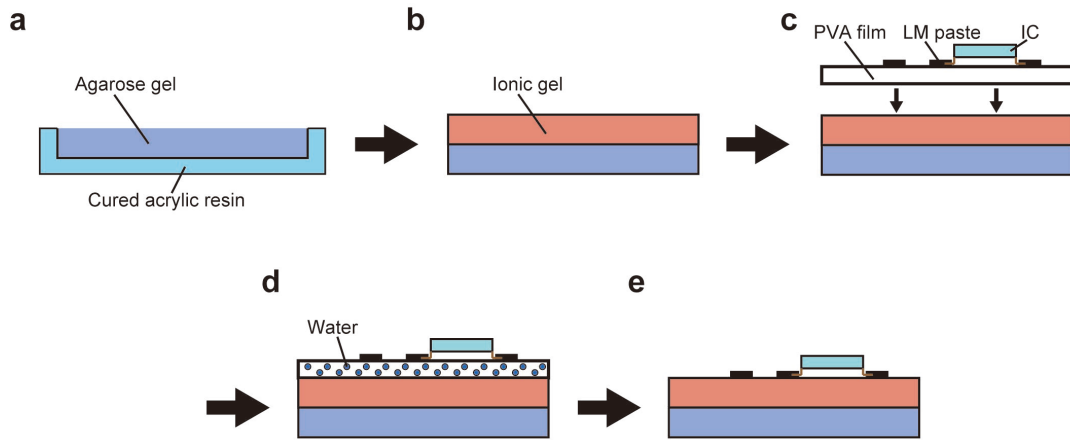


Figure S3. Fabrication process of the temperature measurement device on gels. (a) Agarose gel is poured on the case of acrylic resin. (b) After peeling off the agarose gel from the case, an ionic gel layer is formed on the agarose gel. (c) PVA film containing LM paste electrode and mounted electric components are placed on the ionic gel layer. (d) PVA film is dissolved by water. (e) Mounting of system circuit on the gel.

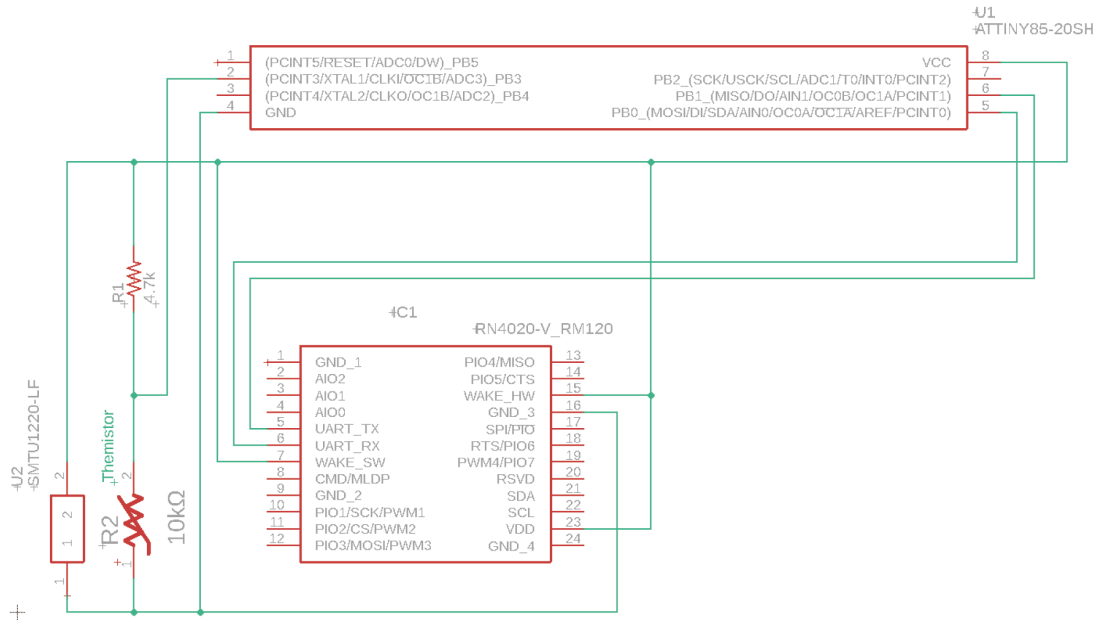


Figure S4. Circuit diagram of the temperature measurement system.

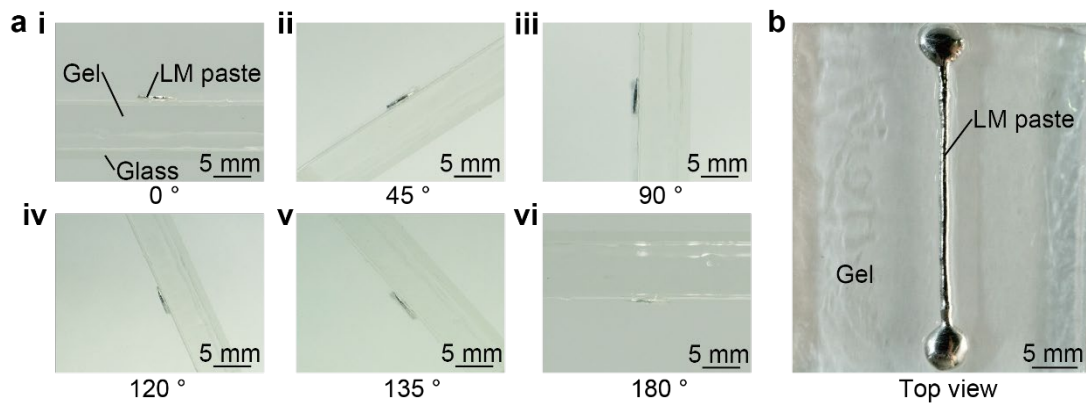


Figure S5. Tilt experiment of LM paste wired on gel. (a) Photographs of LM paste wired on gel, tilted at 0 (i), 45 (ii), 90 (iii), 120 (iv), 135 (v) and 180 degrees (vi). (b) Top view of LM paste wired on gel.

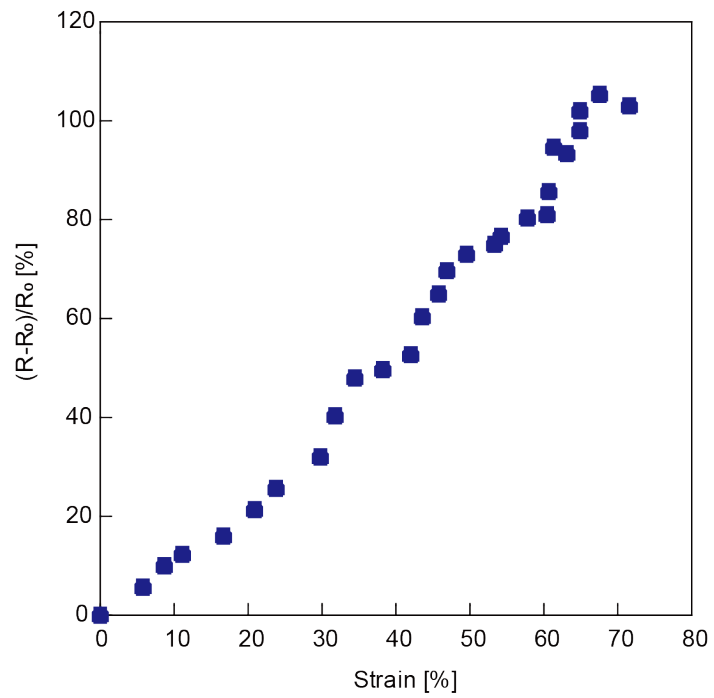


Figure S6. Tensile test using stretchable acrylamide gel.

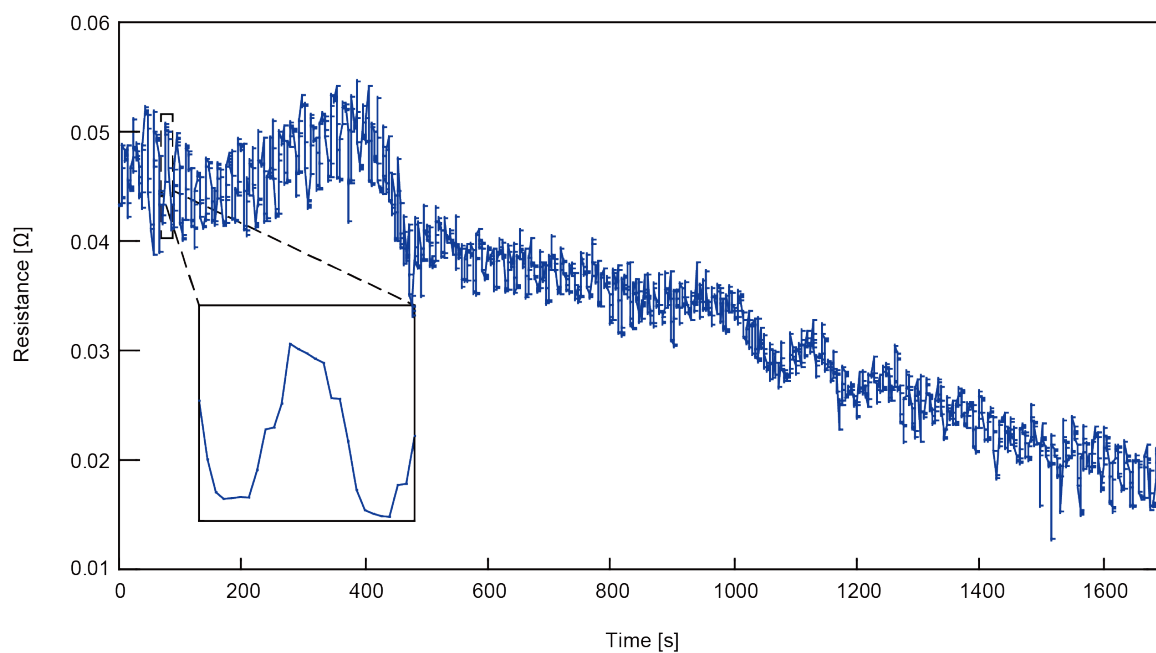


Figure S7. Cyclic stretch-release test.

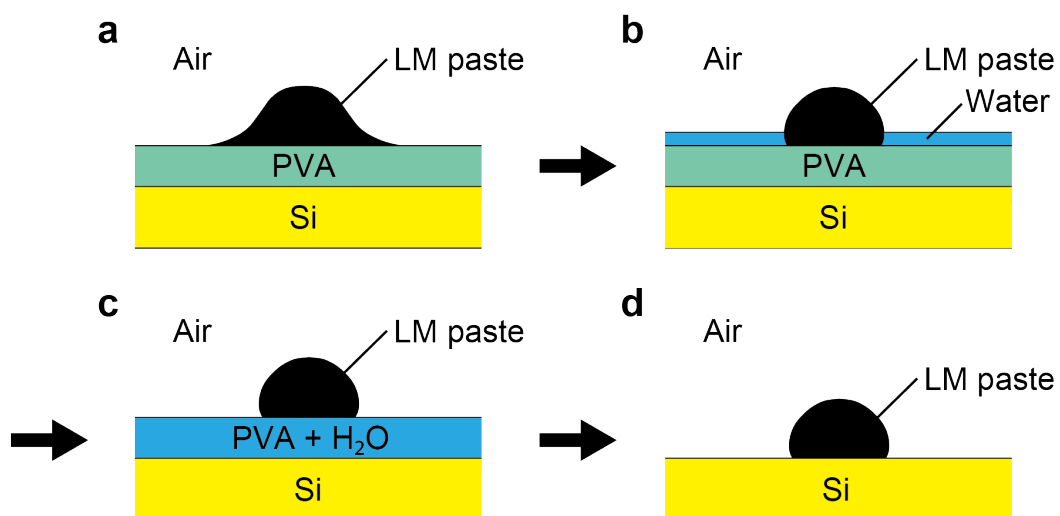


Figure S8. Detail of the mechanism of the transcription process. (a) LM paste wired on the PVA film is placed on the silicon wafer (Si wafer). (b) Water is applied on PVA film. Contact angle changes due to water. (c) Water permeates into PVA film by osmotic pressure (d) LM paste is transferred by melting the PVA film.

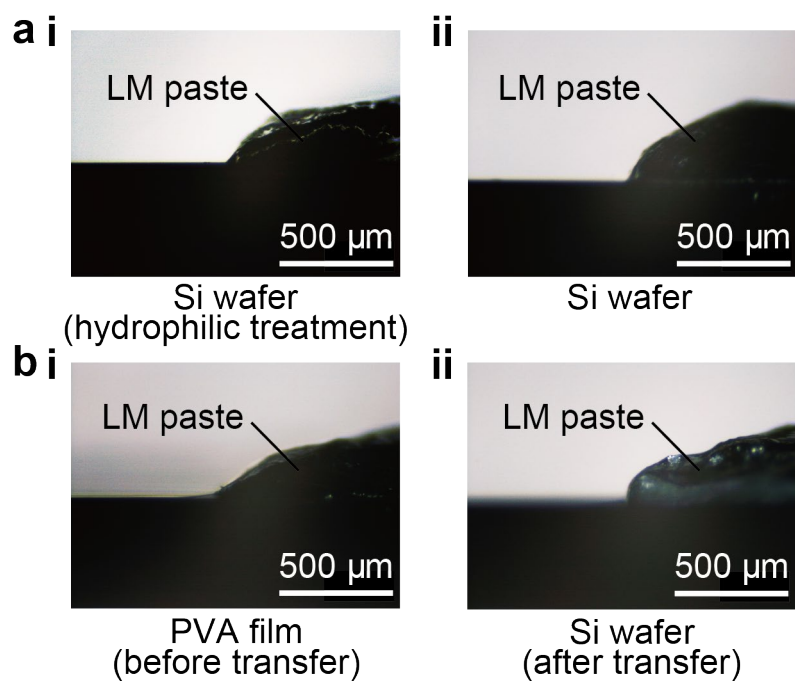


Figure S9. Contact angle between the LM paste and Si wafer. (a) LM paste screen-printed directly on the Si wafer with (i) and without (ii) hydrophilic treatment. (b) LM paste before (i) and after (ii) transferred by the method of this study.

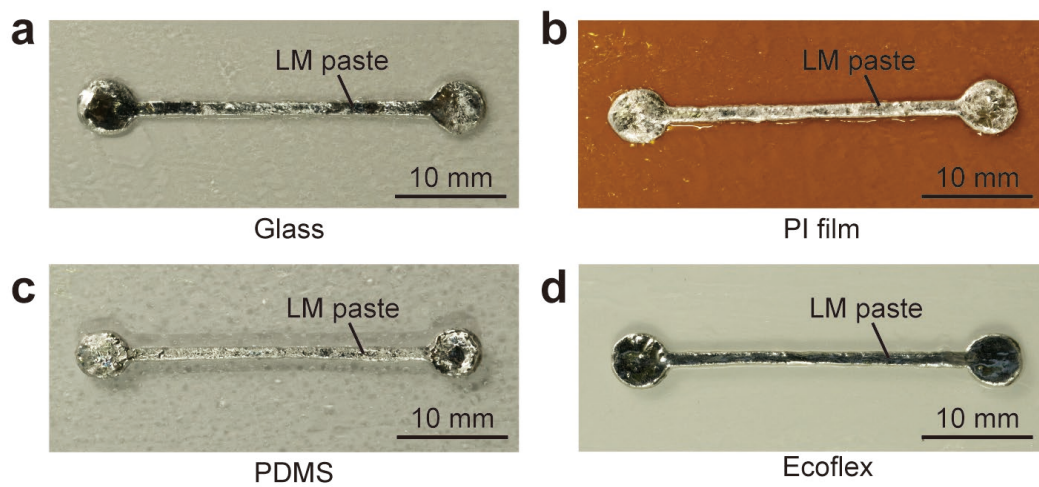


Figure S10. Photographs of LM paste patterns transferred onto hard or rubber substrates. (a) Glass, (b) polyimide, (c) polydimethylsiloxane, and (d) Ecoflex substrates.

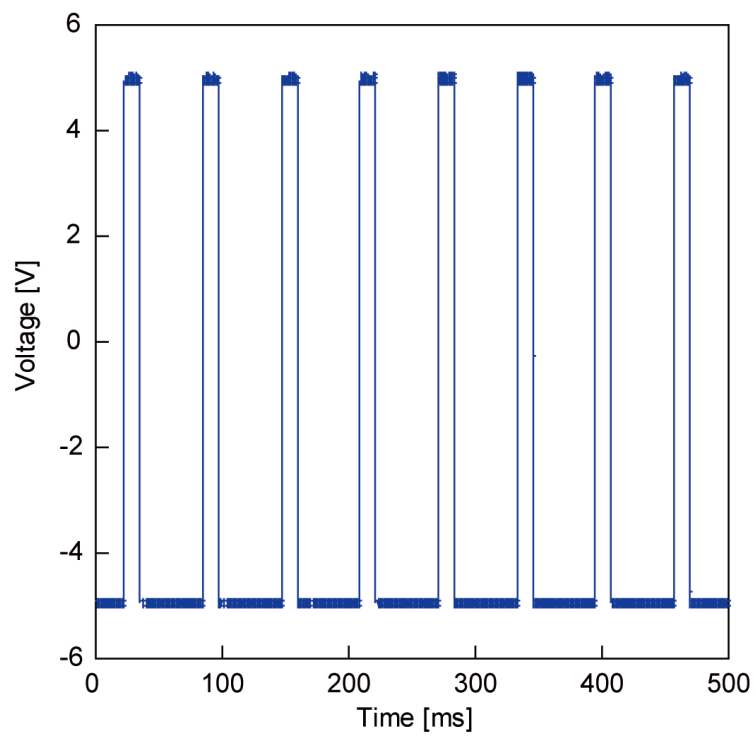


Figure S11. Pulse voltage waveform applied to the vagus nerve of a rat.

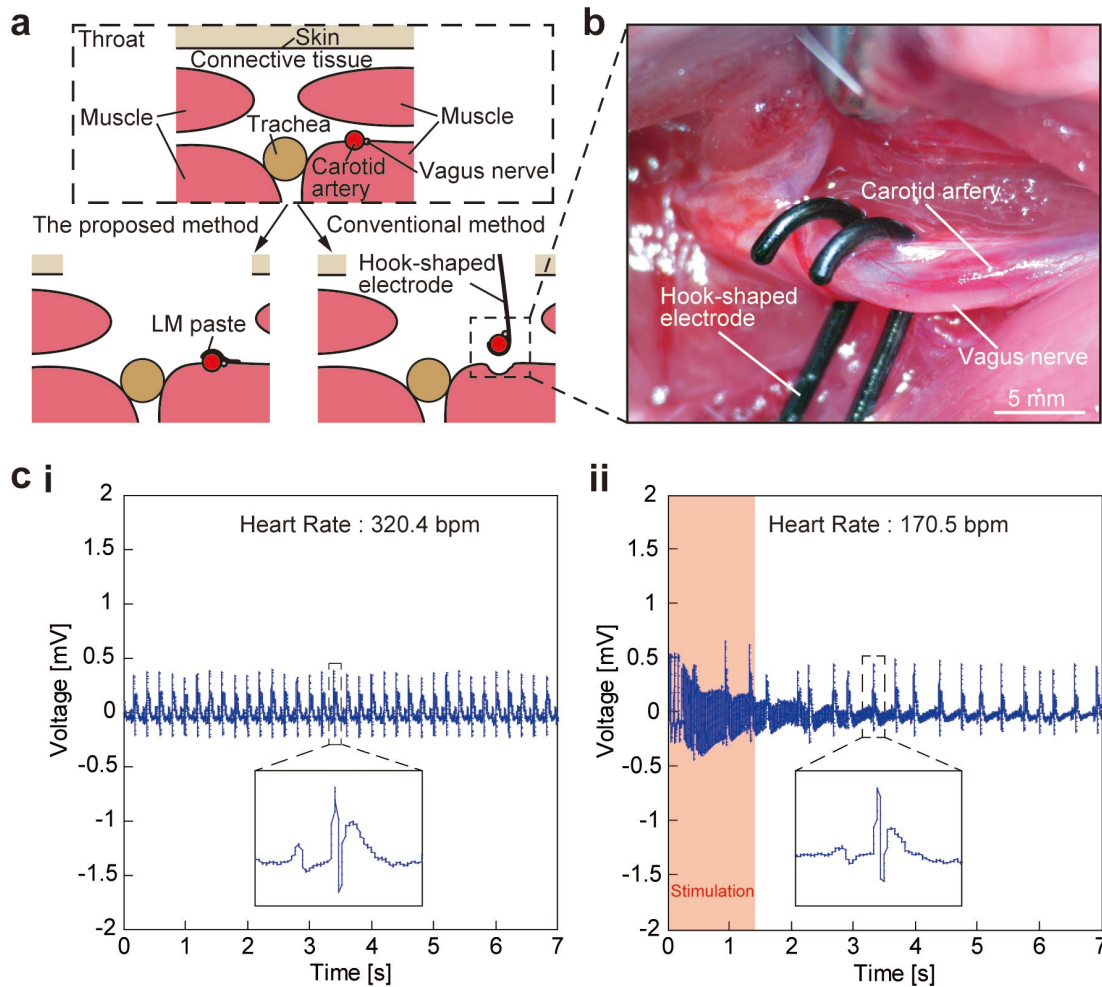


Figure S12. Vagus nerve stimulation in a rat using a hook-shaped electrode. (a) Conceptual diagrams of vagus nerve stimulation using conventional electrodes and the electrodes of this study. (b) Photograph of vagus nerve stimulation using hook-shaped electrode. (c) Electrocardiogram before (i) and after (ii) vagus nerve stimulation.

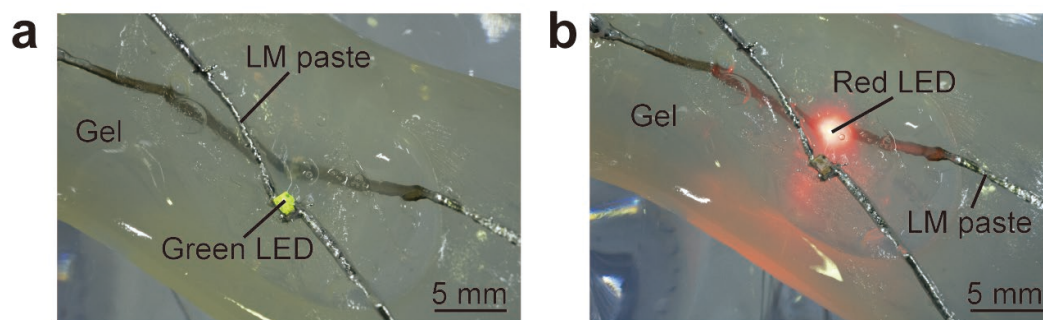


Figure S13. Independent lighting of each light-emitting diode (LED) in the LM paste 3D structure.

(a) Lighting of the green LED on the upper part of the structure. (b) Lighting of the red LED on the bottom layer of the structure.

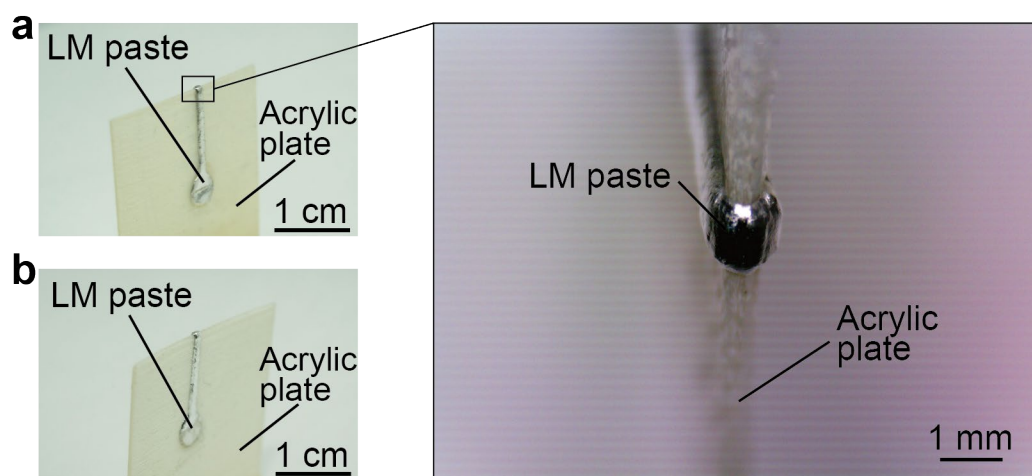


Figure S14. Contact between transferred LM paste and 3D curved surface. (a) Right side. (b) Left side.

Supplementary video 1. Disappearance of PVA film patterned with LM paste by water.